

Current-driven dynamics of frustrated skyrmions in a synthetic antiferromagnetic bilayer

Jing Xia,^{1,*} Xichao Zhang,^{1,*} Motohiko Ezawa,^{2,†} Zhipeng Hou,^{3,4} Wenhong Wang,⁴ Xiaoxi Liu,⁵ and Yan Zhou^{1,‡}

¹*School of Science and Engineering, The Chinese University of Hong Kong, Shenzhen, Guangdong 518172, China*

²*Department of Applied Physics, The University of Tokyo, 7-3-1 Hongo, Tokyo 113-8656, Japan*

³*South China Academy of Advanced Optoelectronics, South China Normal University, Guangzhou 510006, China*

⁴*Beijing National Laboratory for Condensed Matter Physics, Institute of Physics, Chinese Academy of Sciences, Beijing 100190, China*

⁵*Department of Electrical and Computer Engineering, Shinshu University, 4-17-1 Wakasato, Nagano 380-8553, Japan*

(Dated: December 3, 2018)

Magnetic skyrmions can be stabilized and manipulated in frustrated magnets, and are useful for building nonvolatile magnetic memories and logic devices. Here we study the current-driven dynamics of frustrated skyrmions in an antiferromagnetically exchange coupled bilayer system. The bilayer skyrmions consisting of two monolayer skyrmions with opposite skyrmion numbers Q are studied. We show that the in-plane current-driven bilayer skyrmion moves in a straight path (showing no skyrmion Hall effect), while the out-of-plane current-driven bilayer skyrmion moves in a circle path. It is found that the in-plane current-driven mobility of a bilayer skyrmion is much better than the monolayer one at a large ratio of β/α , where α and β denote the damping parameter and non-adiabatic spin transfer torque strength, respectively. Besides, we reveal that one bilayer skyrmion (consisting of monolayer skyrmions with $Q = \pm 2$) can be separated to two bilayer skyrmions (consisting of monolayer skyrmions with $Q = \pm 1$) driven by an out-of-plane current. Our results may be useful for designing skyrmion devices based on frustrated multilayer magnets.

Introduction. The magnetic skyrmion is a topologically non-trivial object¹⁻³, which can be regarded as quasi-particles⁴ and promises advanced electronic and spintronic applications⁵⁻⁸. For examples, recent theoretical and experimental studies have suggested that skyrmions can be used as building blocks for racetrack-type memories⁹⁻¹², logic computing devices¹³, and bio-inspired applications¹⁴⁻¹⁷. The magnetic skyrmion was first experimentally observed in ferromagnetic (FM) materials with Dzyaloshinskii-Moriya (DM) interactions almost ten years ago in 2009¹⁸, where the DM interaction is an essential energy term stabilizing skyrmion textures¹⁸⁻²⁰. The DM interaction can also be induced at the interface between the heavy metal and ferromagnet²¹, which promotes recent studies of skyrmions in magnetic bilayer and multilayer structures^{3,22-28}.

However, by inducing the DM interaction is not the only way to stabilize skyrmions. Most recently, theoretical and experimental studies have demonstrated that skyrmions can be stabilized in frustrated magnets even in the absence of DM interaction²⁹⁻⁴¹, where skyrmion textures are stabilized by competing exchange interactions^{30,31,34,35}. Frustrated skyrmions have many unique physical properties compared with their counterparts in DM ferromagnets. For examples, both skyrmions and antiskyrmions can exist in a frustrated magnet as metastable states^{30,31,34,35}. The frustrated skyrmions with skyrmion number of $Q = 1$ can merge and form skyrmions with higher skyrmion number of $Q = 2$ ³⁵. Besides, the center-of-mass dynamics of a frustrated skyrmion is coupled to its helicity dynamics^{30,31,34}, which results in the rotational motion of a skyrmion^{31,35}. Therefore, frustrated skyrmions can be used as information carriers, which have multiple degrees of freedom that can be utilized to store information^{30,31,34,35}. Indeed, a recent experimental work demonstrates that the helicity of a frustrated skyrmion can be switched by an electric current pulse⁴², which offers the possibility to design helicity-based skyrmion memories. So far, most studies on frustrated skyrmions are focused on their dynamics in the monolayer

system, while bilayer and multilayer systems play an important role in developing nanoscale devices^{3,22-28,43,44}.

In this Letter, we report the dynamics of frustrated skyrmions with $Q = \pm 1$ and ± 2 in an antiferromagnetically exchange coupled bilayer system driven by either an in-plane or an out-of-plane spin current. The antiferromagnetically exchange coupled bilayer system can be regarded as a synthetic antiferromagnet, which is promising for building racetrack-type memories^{26,43}. We also numerically investigate the current-induced separation of a frustrated skyrmion in the synthetic antiferromagnetic (AFM) bilayer system. We show that the current-driven frustrated skyrmions in the synthetic AFM bilayer system have better mobility than the monolayer skyrmions.

Methods. We consider two frustrated FM layers with competing Heisenberg exchange interactions based on the J_1 - J_2 - J_3 model on a simple square lattice^{31,35}. As shown in Fig. 1(a), the two frustrated FM layers are coupled by an AFM interfacial exchange coupling, which can be realized by utilizing the Ruderman-Kittel-Kasuya-Yosida (RKKY) interaction^{26,43,44}. For example, the interlayer AFM coupling between two FM layers can be mediated by an ultrathin metallic spacer layer^{43,44}. We assume the background magnetization direction in the bottom FM layer to be pointing along the $+z$ direction. The total Hamiltonian for the synthetic AFM bilayer is given in Ref. 45. The simulation is performed by using the standard micromagnetic simulator Object Oriented MicroMagnetic Framework (OOMMF)⁴⁶ with our home-made extension modules for the J_1 - J_2 - J_3 classical Heisenberg model^{31,35}, where the time-dependent spin dynamics is described by the Landau-Lifshitz-Gilbert (LLG) equation (see Ref. 45 for modeling details and parameters).

We consider two geometries for the injection of spin-polarized current. For the current-in-plane (CIP) geometry, an in-plane spin current is injected to both top and bottom FM layers, and the adiabatic (τ_1) and non-adiabatic (τ_2) spin

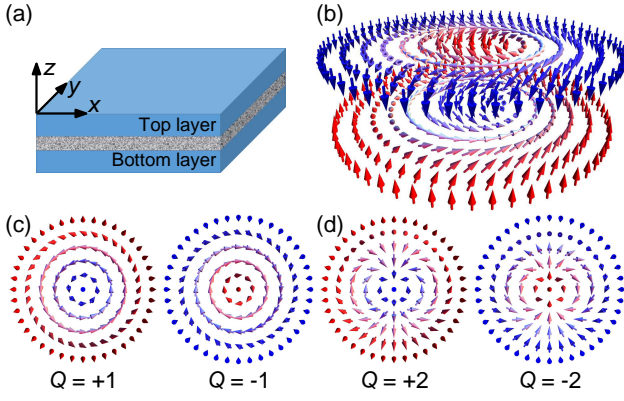


FIG. 1. (a) Schematic of the simulated synthetic AFM bilayer model. Namely, the top and bottom FM layers are coupled via an AFM interfacial exchange coupling. (b) Illustration of the synthetic AFM bilayer skyrmion. (c) Illustration of the monolayer skyrmion with $Q = \pm 1$. (d) Illustration of the monolayer skyrmion with $Q = \pm 2$. The arrows represent the magnetization directions. The out-of-plane component of magnetization (m_z) is color coded: blue is into the plane, red is out of the plane, white is in-plane.

transfer torque (STT) terms are considered, given as

$$\tau_1 = u \left(\mathbf{m} \times \frac{\partial \mathbf{m}}{\partial x} \times \mathbf{m} \right), \tau_2 = -\beta u \left(\mathbf{m} \times \frac{\partial \mathbf{m}}{\partial x} \right), \quad (1)$$

where \mathbf{m} represents the normalized spin, $u = \left| \frac{\gamma_0 \hbar}{\mu_0 e} \right| \frac{jP}{2M_S}$ is the STT coefficient and β is the strength of the non-adiabatic STT torque. \hbar is the reduced Planck constant, e is the electron charge, j is the applied driving current density, $P = 0.4$ is the spin polarization rate⁹, and M_S is the saturation magnetization. For the current-perpendicular-to-plane (CPP) geometry, an out-of-plane spin current is only injected to the bottom FM layer, which can be realized by harnessing the spin Hall effect in a heavy-metal substrate underneath the bottom FM layer²⁷. In such a case, the damping-like STT term is considered, given as

$$\tau_d = \frac{u}{a} (\mathbf{m} \times \mathbf{p} \times \mathbf{m}), \quad (2)$$

where $a = 0.4$ nm is the thickness of a single FM layer and $\mathbf{p} = +\hat{y}$ stands for the unit spin polarization direction. Note that we ignore the field-like STT term for simplicity as its contribution to the skyrmion dynamics is minor. For the CPP geometry, we set $P = 0.1$, which is a typical value of spin Hall angle^{10,27}. The skyrmion number in a single FM layer is defined by $Q = -\int d^2\mathbf{r} \cdot \mathbf{m} \cdot (\partial_x \mathbf{m} \times \partial_y \mathbf{m}) / 4\pi$. The internal structure of a skyrmion is also described by its helicity number $\eta = [0, 2\pi)$, of which the definition is given in Refs. 2 and 47.

Skyrmions driven by an in-plane current. We first study in-plane current-driven skyrmions in a synthetic AFM bilayer [see Fig. 1(a)]. At first, a bilayer skyrmion is relaxed in a synthetic AFM bilayer, which consists of a top skyrmion with $Q = -1$ and $\eta = 3\pi/2$ and a bottom skyrmion with $Q = +1$ and $\eta = \pi/2$ [see Fig. 1(b)]. The monolayer skyrmion structures with $Q = \pm 1$ are illustrated in Fig. 1(c). In this work, we refer to this bilayer skyrmion as a bilayer skyrmion with

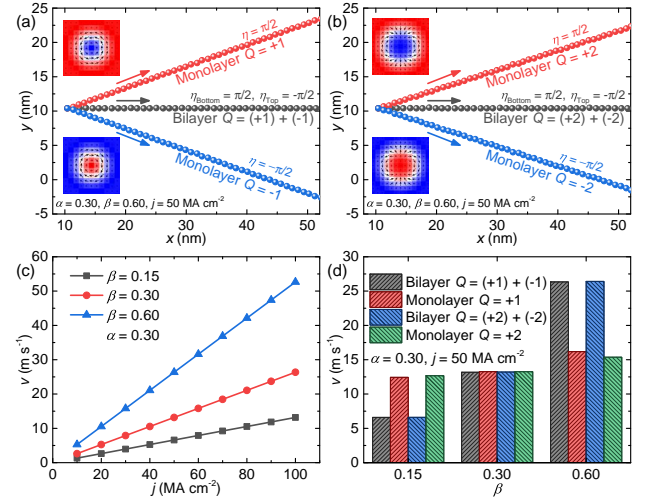


FIG. 2. (a) Trajectories of monolayer and bilayer skyrmions with $Q = \pm 1$ driven by an in-plane current at $\alpha = \beta/2 = 0.30$. Arrows denote the motion direction. Insets are the top-view snapshots of simulated skyrmions with $Q = \pm 1$ and $\eta = \pm\pi/2$. (b) Trajectories of monolayer and bilayer skyrmions with $Q = \pm 2$ driven by an in-plane current. Insets are the top-view snapshots of simulated skyrmions with $Q = \pm 2$ and $\eta = \pm\pi/2$. (c) Bilayer skyrmion ($Q = \pm 1$ and ± 2) velocity as a function of in-plane driving current density. (d) Comparison of the monolayer skyrmion velocity and bilayer skyrmion velocity induced by an in-plane current.

$Q = \pm 1$. The top and bottom skyrmions are strongly coupled as a result of the AFM interfacial exchange coupling. The relaxed diameter of the bilayer skyrmion with $Q = \pm 1$ equals 2 nm. Note that the diameters of the relaxed skyrmions in monolayer and bilayer systems are identical. An in-plane spin current is then injected into both top and bottom FM layers (i.e., with the CIP geometry), which drives the bilayer skyrmion into motion. We also study the skyrmion motion in a single FM monolayer for the purpose of comparison.

Figure 1 shows the trajectories of the monolayer and bilayer skyrmions at the damping parameter $\alpha = \beta/2 = 0.3$. It is found that the bilayer skyrmion with $Q = \pm 1$ straightly moves along the $+x$ direction without showing a transverse shift. However, the monolayer skyrmions with $Q = +1$ and $Q = -1$ show transverse shifts toward the $+y$ and $-y$ directions, respectively. The reason is that the monolayer skyrmion experiences a topological Magnus force^{26–28}, which leads to its transverse shift. Since the directions of Magnus forces acted on monolayer skyrmions with $Q = +1$ and $Q = -1$ are opposite, the bilayer skyrmion consisting of a bottom monolayer skyrmion with $Q = +1$ and a top monolayer skyrmion with $Q = -1$ experiences zero net Magnus force and thus can move in a straight path. It is worth mentioning that the transverse shift of skyrmion is referred as the skyrmion Hall effect, which has been directly observed in experiments^{27,28}. A previous study has reported the skyrmion Hall effect of the monolayer skyrmion driven by an in-plane current can be eliminated only when $\alpha = \beta$ ⁴⁸, which is difficult to be realized in real materials. However, the bilayer skyrmion driven by an in-plane current shows no skyrmion Hall effect even

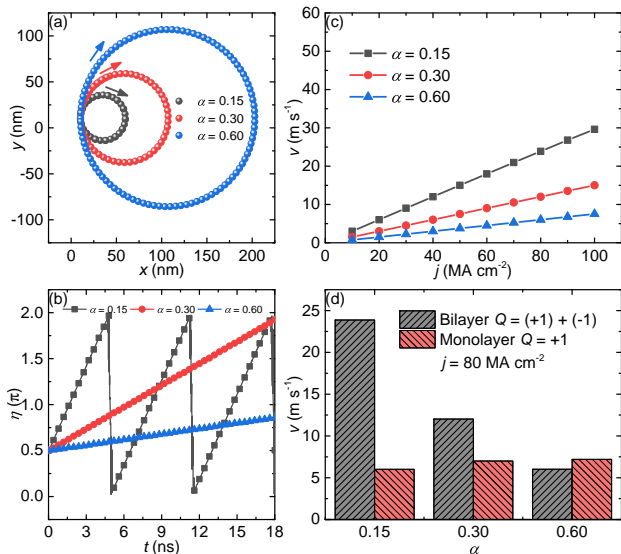


FIG. 3. (a) Trajectories of bilayer skyrmions with $Q = \pm 1$ driven by an out-of-plane current. Arrows denote the motion direction. (b) Helicity as a function of time during the motion of bilayer skyrmions with $Q = \pm 1$, corresponding to (a). For the bilayer skyrmion, the helicity of the skyrmion in bottom FM layer is shown. (c) Bilayer skyrmion ($Q = \pm 1$) velocity as a function of out-of-plane driving current density. (d) Comparison of the monolayer skyrmion velocity and bilayer skyrmion velocity induced by an out-of-plane current.

when $\alpha \neq \beta$, which is useful for building racetrack-type devices^{10,26}.

As shown in Fig. 2(b), we also simulate the motion of a bilayer skyrmion with $Q = \pm 2$, which consists of a bottom monolayer skyrmion with $Q = +2$ and $\eta = \pi/2$ and a top monolayer skyrmion with $Q = -2$ and $\eta = 3\pi/2$ [see Fig. 1(d)]. Similarly, the bilayer skyrmion with $Q = \pm 2$ driven by an in-plane current also straightly moves along the $+x$ direction. The monolayer skyrmions with $Q = +2$ and $Q = -2$ show transverse shifts toward the $+y$ and $-y$ directions, respectively. Note that the relaxed size of skyrmions with $Q = \pm 2$ equals 2.8 nm, which is slightly larger than that of skyrmions with $Q = \pm 1$.

Figure 2(c) shows the bilayer skyrmion velocity v as a function of in-plane driving current density j for $\alpha = 0.3$ and $\beta = 0.15 \sim 0.60$. It should be noted that the $v - j$ relation of the bilayer skyrmion with $Q = \pm 1$ is identical to that of the bilayer skyrmion with $Q = \pm 2$ at a given α and β . For both bilayer skyrmions with $Q = \pm 1$ and $Q = \pm 2$, the velocity increases linearly with the in-plane driving current density. At certain values of α and j , larger β will result in larger velocity of the bilayer skyrmion. By comparing the velocities of bilayer and monolayer skyrmions at certain values of α and j , it is found that bilayer skyrmions move faster than monolayer skyrmions when $\alpha < \beta$, while bilayer skyrmions move slower than monolayer skyrmions when $\alpha > \beta$. When $\alpha = \beta$, the velocities for bilayer and monolayer skyrmions are almost identical. It is worth mentioning that several experiments suggest that β is considerably larger than α (i.e., $\alpha \ll \beta$)^{49,50}, which means the mobility of bilayer skyrmion is better than

that of monolayer skyrmion. The monolayer skyrmion speed is proportional to β/α in the absence of the skyrmion Hall effect⁹, which is the same case for the bilayer skyrmion studied here.

Skyrmions driven by an out-of-plane current. We also study out-of-plane current-driven skyrmions in a synthetic AFM bilayer. Namely, a spin current is perpendicularly injected into the bottom FM layer (i.e., with the CPP geometry), which drives the skyrmion in the bottom FM layer into motion. The skyrmion in the top FM layer is simultaneously dragged into motion as the bottom and top skyrmions of a synthetic AFM bilayer skyrmion are strongly coupled. We first study the bilayer skyrmion with $Q = \pm 1$ as well as monolayer skyrmions with $Q = +1$ and $Q = -1$ driven by an out-of-plane current.

As shown in Fig. 3, the dynamics of a bilayer skyrmion with $Q = \pm 1$ and its monolayer counterparts (see Ref. 45) driven by an out-of-plane current are in stark contrast to the case driven by an in-plane current. It can be seen that the bilayer skyrmion with $Q = \pm 1$ [see Fig. 3(a)] and monolayer skyrmions with $Q = +1$ and $Q = -1$ (see Ref. 45) driven by an out-of-plane current move in a circle path. The bilayer skyrmion with $Q = \pm 1$ moves in the clockwise direction, while the monolayer skyrmions with $Q = +1$ and $Q = -1$ move in the counterclockwise and clockwise directions, respectively. As pointed out in Ref. 31, the motion direction depends on the skyrmion helicity. For both the bilayer and monolayer skyrmions, the diameter of circle trajectory increases with increasing α . Under the same out-of-plane driving current density and α , the diameter of the bilayer skyrmion trajectory is significantly larger than that of monolayer skyrmion trajectory, which means the frustrated skyrmion can be delivered farther in the bilayer system driven by an out-of-plane current.

On the other hand, the helicity numbers η of bilayer skyrmion with $Q = \pm 1$ [see Fig. 3(b)] and monolayer skyrmions with $Q = +1$ and $Q = -1$ (see Ref. 45) driven by an out-of-plane current are coupled to their center-of-mass dynamics. Namely, the helicity number η changes linearly with time during the motion of skyrmions. Such a phenomenon has been reported for monolayer skyrmions in Ref. 31, and we show that it also happens for bilayer skyrmions with $Q = \pm 1$. As pointed out in Ref. 31, the frustrated monolayer skyrmion has a translational mode and a rotational mode, which can be excited and hybridized by the damping-like STT due to the spin Hall effect. Namely, when the skyrmion in the bottom FM layer is driven by the damping-like STT, it moves along a circle with rotating helicity. At the same time, it drives the skyrmion in the top FM layer into circular motion with rotating helicity due to the AFM interlayer coupling.

Figure 3(c) shows the velocity of the bilayer skyrmion with $Q = \pm 1$ as a function of out-of-plane driving current density. At a given α , the velocity of bilayer skyrmion with $Q = \pm 1$ increases linearly with driving current density j . At a given j , the velocity of bilayer skyrmion with $Q = \pm 1$ is inversely proportional to the value of α . By comparing Fig. 2(d) and Fig. 3(c) at same j and α , it is found that the bilayer skyrmion with $Q = \pm 1$ driven by an in-plane current can move much faster than the one driven by an out-of-plane current if the

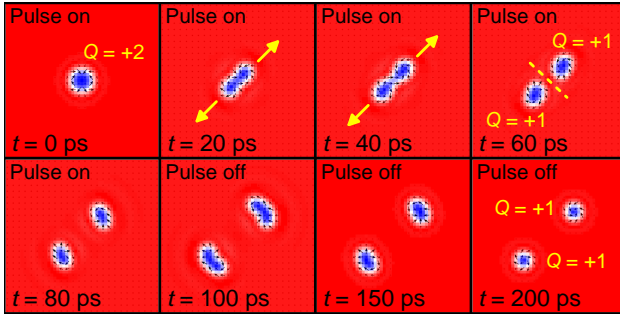


FIG. 4. Out-of-plane current-induced separation of one bilayer skyrmion (consisting of two monolayer skyrmions with $Q = \pm 2$) to two bilayer skyrmions (consisting of monolayer skyrmions with $Q = \pm 1$). Snapshots are top views of the bottom FM layer. Here, a current pulse of $j = 400 \text{ MA cm}^{-2}$ is applied for 100 ps to force the separation.

value of β is large. For example, when $j = 100 \text{ MA cm}^{-2}$ and $\alpha = 0.3$, the bilayer skyrmion with $Q = \pm 1$ driven by an in-plane current can reach a velocity of $v = 53 \text{ m s}^{-1}$ at $\beta = 0.6$, while the one driven by an out-of-plane current only reaches a velocity of $v = 15 \text{ m s}^{-1}$. However, it should be noted that the driving force provided by the in-plane current is larger than that provided by the out-of-plane current at the same j in this work, as the CIP spin-polarization rate is four times larger than the CPP spin Hall angle. The bilayer skyrmion driven by the out-of-plane current can move faster when the value of the spin Hall angle is increased.

Besides, by comparing the velocities of bilayer skyrmion with $Q = \pm 1$ and monolayer skyrmions with $Q = +1$ and $Q = -1$ at a given j [see Fig. 3(d)], it is found that the bilayer skyrmion velocity remarkably decreases with increasing α , while the monolayer skyrmion velocity slightly increases with increasing α . The significant decrease of bilayer skyrmion velocity with increasing α may be caused by the enhancement of the dissipative force provided by the skyrmion in the top FM layer due to the increasing damping parameter. The bilayer skyrmion velocity is much larger than monolayer skyrmion velocity at small α (e.g., $\alpha = 0.15$), while it is smaller than monolayer skyrmion velocity at large α (e.g., $\alpha = 0.60$).

We continue to study the bilayer skyrmion with $Q = \pm 2$ and monolayer skyrmions with $Q = +2$ and $Q = -2$ driven by an out-of-plane current. As shown in Fig. 4, it is found that the bilayer skyrmion with $Q = \pm 2$ does not move toward a certain direction when an out-of-plane current is applied. Instead, it is elongated and then separated to two bilayer skyrmions with $Q = \pm 1$. The reason is that the bilayer skyrmion with $Q = \pm 2$ is topologically equal to a combination of two bilayer skyrmions with $Q = \pm 1$ and opposite helicity numbers. Such two bilayer skyrmions with $Q = \pm 1$ tend to move along opposite directions upon the application of the out-of-plane current, as indicated by yellow arrows in Fig. 4. Similarly, when an out-of-plane current is

applied, the monolayer skyrmion with $Q = +2$ is separated to two monolayer skyrmions with $Q = +1$ and the monolayer skyrmion with $Q = -2$ is separated to two monolayer skyrmions with $Q = -1$ (see Ref. 45). The most obvious difference between the out-of-plane current-induced separation of a bilayer skyrmion with $Q = \pm 2$ and the separation of a monolayer skyrmion with $Q = +2$ or $Q = -2$ is that the separation of a monolayer skyrmion is accompanied with an obvious clockwise or counterclockwise rotation of the skyrmion structure. The reason is that the out-of-plane current-induced circular motion diameter of the monolayer skyrmion with $Q = +1$ or $Q = -1$ is much smaller than that of the bilayer skyrmion with $Q = \pm 1$. Hence, the separation of the monolayer skyrmion with $Q = \pm 2$ shows very obvious rotation caused by the circular motion of monolayer skyrmions with $Q = +1$ and $Q = -1$. Note that if the an out-of-plane current is applied after the separation of the bilayer skyrmion with $Q = \pm 2$, it will also drive the bilayer skyrmions with $Q = \pm 1$ into motion along a large circle [see Fig. 3(a)].

Conclusion. In conclusion, we have studied the dynamics of frustrated bilayer skyrmions driven by an in-plane or out-of-plane spin-polarized current in a synthetic AFM bilayer. It is found that the bilayer skyrmion with $Q = \pm 1$ or $Q = \pm 2$ moves in a straight path driven by an in-plane current, while the bilayer skyrmion with $Q = \pm 1$ moves in a circle path driven by an out-of-plane current. Therefore, the bilayer skyrmion is promising for building racetrack-type applications, as it shows no skyrmion Hall effect and can be delivered in a straight line even when $\alpha \neq \beta$. At same j and α , the mobility of the bilayer skyrmion with $Q = \pm 1$ driven by an in-plane current is better than that driven by an out-of-plane current at large β . The out-of-plane current can lead to the separation of a bilayer skyrmion with $Q = \pm 2$ to two bilayer skyrmions with $Q = \pm 1$. The separation of a bilayer skyrmion with $Q = \pm 2$ does not show the rotation of skyrmion structure, while the monolayer skyrmion with $Q = +2$ or $Q = -2$ is rotating until it is separated to two monolayer skyrmions with $Q = +1$ or $Q = -1$. Our results are useful for understanding bilayer skyrmion physics in frustrated magnets and could provide guidelines for building skyrmion devices.

Acknowledgments. This work was supported by the Presidential Postdoctoral Fellowship and the President's Fund of CUHKSZ, the Shenzhen Fundamental Research Fund (Grant Nos. JCYJ20160331164412545 and JCYJ20170410171958839), the National Natural Science Foundation of China (Grant Nos. 11574137, 11604148 and 11874410), the National Key R&D Program of China (Grant Nos. 2017YFA0303202 and 2017YFA206303), the Key Research Program of the Chinese Academy of Sciences (Grant No. KJZD-SW-M01), the Grants-in-Aid for Scientific Research from JSPS KAKENHI (Grant Nos. JP18H03676, JP17K05490, JP15H05854 and JP17K19074), and CREST, JST (Grant Nos. JPMJCR1874 and JPMJCR16F1).

- * These authors contributed equally to this work.
- † E-mail: ezawa@ap.t.u-tokyo.ac.jp
- ‡ E-mail: zhouyan@cuhk.edu.cn
- ¹ U. K. Röbber, A. N. Bogdanov and C. Pfeleiderer, *Nature* **442**, 797 (2006).
 - ² N. Nagaosa and Y. Tokura, *Nat. Nanotech.* **8**, 899 (2013).
 - ³ W. Jiang, G. Chen, K. Liu, J. Zang, S. G. Velthuis and A. Hoffmann, *Phys. Rep.* **704**, 1 (2017).
 - ⁴ S.-Z. Lin, C. Reichhardt, C. D. Batista and A. Saxena, *Phys. Rev. B* **87**, 214419 (2013).
 - ⁵ A. Fert, N. Reyren and V. Cros, *Nat. Rev. Mater.* **2**, 17031 (2017).
 - ⁶ G. Finocchio, F. Büttner, R. Tomasello, M. Carpentieri and M. Kläui, *J. Phys. D: Appl. Phys.* **49**, 423001 (2016).
 - ⁷ W. Kang, Y. Huang, X. Zhang, Y. Zhou and W. Zhao, *Proc. IEEE* **104**, 2040-2061 (2016).
 - ⁸ Y. Zhou, *Natl. Sci. Rev.* **6**, 1 (2018).
 - ⁹ J. Sampaio, V. Cros, S. Rohart, A. Thiaville and A. Fert, *Nat. Nanotech.* **8**, 839 (2013).
 - ¹⁰ R. Tomasello, E. Martinez, R. Zivieri, L. Torres, M. Carpentieri and G. Finocchio, *Sci. Rep.* **4**, 6784 (2014).
 - ¹¹ G. Yu, P. Upadhyaya, Q. Shao, H. Wu, G. Yin, X. Li, C. He, W. Jiang, X. Han, P. K. Amiri and K. L. Wang, *Nano Lett.* **17**, 261 (2017).
 - ¹² J. Müller, *New J. Phys.* **19** 025002, (2017).
 - ¹³ X. Zhang, M. Ezawa and Y. Zhou, *Sci. Rep.* **5**, 9400 (2015).
 - ¹⁴ Y. Huang, W. Kang, X. Zhang, Y. Zhou and W. Zhao, *Nanotechnology* **28**, 08LT02 (2017).
 - ¹⁵ S. Li, W. Kang, Y. Huang, X. Zhang, Y. Zhou and W. Zhao, *Nanotechnology* **28**, 31LT01 (2017).
 - ¹⁶ D. Prychynenko, M. Sitte, K. Litzius, B. Krüger, G. Bourianoff, M. Kläui, J. Sinova and K. Everschor-Sitte, *Phys. Rev. Appl.* **9**, 014034 (2018).
 - ¹⁷ G. Bourianoff, D. Pinna, M. Sitte and K. Everschor-Sitte, *AIP Adv.* **8**, 055602 (2018).
 - ¹⁸ S. Mühlbauer, B. Binz, F. Jonietz, C. Pfeleiderer, A. Rosch, A. Neubauer, R. Georgii and P. Böni, *Science* **323**, 915 (2009).
 - ¹⁹ X. Z. Yu, Y. Onose, N. Kanazawa, J. H. Park, J. H. Han, Y. Matsui, N. Nagaosa and Y. Tokura, *Nature* **465**, 901 (2010).
 - ²⁰ H. Du, R. Che, L. Kong, X. Zhao, C. Jin, C. Wang, J. Yang, W. Ning, R. Li, C. Jin, X. Chen, J. Zang, Y. Zhan and M. Tian, *Nat. Commun.* **6**, 8504 (2015).
 - ²¹ H. Yang, A. Thiaville, S. Rohart, A. Fert and M. Chshiev, *Phys. Rev. Lett.* **115**, 267210 (2015).
 - ²² S. Woo, K. Litzius, B. Kruger, M.-Y. Im, L. Caretta, K. Richter, M. Mann, A. Krone, R. M. Reeve, M. Weigand, P. Agrawal, I. Limesh, M.-A. Mawass, P. Fischer, M. Klauai and G. S. D. Beach, *Nat. Mater.* **15**, 501 (2016).
 - ²³ C. Moreau-Luchaire, C. Moutafis, N. Reyren, J. Sampaio, C. A. F. Vaz, N. Van Horne, K. Bouzehouane, K. Garcia, C. Deranlot, P. Warnicke, P. Wohlhüter, J.-M. George, M. Weigand, J. Raabe, V. Cros and A. Fert, *Nat. Nanotech.* **11**, 444 (2016).
 - ²⁴ S. D. Pollard, J. A. Garlow, J. Yu, Z. Wang, Y. Zhu and H. Yang, *Nat. Commun.* **8**, 14761 (2017).
 - ²⁵ S. Woo, K. M. Song, X. Zhang, M. Ezawa, Y. Zhou, X. Liu, M. Weigand, S. Finizio, J. Raabe, M.-C. Park, K.-Y. Lee, J. W. Choi, B.-C. Min, H. C. Koo and J. Chang, *Nat. Electron.* **1**, 288 (2018).
 - ²⁶ X. Zhang, Y. Zhou and M. Ezawa, *Nat. Commun.* **7**, 10293 (2016).
 - ²⁷ W. Jiang, X. Zhang, G. Yu, W. Zhang, X. Wang, M. Benjamin Jungfleisch, J. E. Pearson, X. Cheng, O. Heinonen, K. L. Wang, Y. Zhou, A. Hoffmann and S. G. E. Velthuis, *Nat. Phys.* **13**, 162 (2017).
 - ²⁸ K. Litzius, I. Limesh, B. Kruger, P. Bassirian, L. Caretta, K. Richter, F. Büttner, K. Sato, O. A. Tretiakov, J. Forster, R. M. Reeve, M. Weigand, I. Bykova, H. Stoll, G. Schutz, G. S. D. Beach and M. Klauai, *Nat. Phys.* **13**, 170 (2017).
 - ²⁹ T. Okubo, S. Chung and H. Kawamura, *Phys. Rev. Lett.* **108**, 017206 (2012).
 - ³⁰ A. O. Leonov and M. Mostovoy, *Nat. Commun.* **6**, 8275 (2015).
 - ³¹ S.-Z. Lin and S. Hayami, *Phys. Rev. B* **93**, 064430 (2016).
 - ³² S. Hayami, S.-Z. Lin and C. D. Batista, *Phys. Rev. B* **93**, 184413 (2016).
 - ³³ L. Rózsa, A. Deák, E. Simon, R. Yanes, L. Udvardi, L. Szunyogh and U. Nowak, *Phys. Rev. Lett.* **117**, 157205 (2016).
 - ³⁴ A. O. Leonov and M. Mostovoy, *Nat. Commun.* **8**, 14394 (2017).
 - ³⁵ X. Zhang, J. Xia, Y. Zhou, X. Liu, H. Zhang and M. Ezawa, *Nat. Commun.* **8**, 1717 (2017).
 - ³⁶ H. Y. Yuan, O. Gomonay and M. Kläui, *Phys. Rev. B* **96**, 134415 (2017).
 - ³⁷ L. Rózsa, K. Palotás, A. Deák, E. Simon, R. Yanes, L. Udvardi, L. Szunyogh and U. Nowak, *Physical Review B* **95**, 094423 (2017).
 - ³⁸ Y. A. Kharkov, O. P. Sushkov and M. Mostovoy, *Phys. Rev. Lett.* **119**, 207201 (2017).
 - ³⁹ Z. Hou, W. Ren, B. Ding, G. Xu, Y. Wang, B. Yang, Q. Zhang, Y. Zhang, E. Liu, F. Xu, W. Wang, G. Wu, X. Zhang, B. Shen and Z. Zhang, *Adv. Mater.* **29**, 1701144 (2017).
 - ⁴⁰ P. Sutcliffe, *Phys. Rev. Lett.* **118**, 247203 (2017).
 - ⁴¹ J. J. Liang, J. H. Yu, J. Chen, M. H. Qin, M. Zeng, X. B. Lu, X. S. Gao and J. Liu, *New J Phys.* **20**, 053037 (2018).
 - ⁴² Z. P. Hou (private communication).
 - ⁴³ S.-H. Yang, K.-S. Ryu and S. Parkin, *Nat. Nanotech.* **10**, 221 (2015).
 - ⁴⁴ A. Prudnikov, M. Li, M. D. Graef and V. Sokalski, *IEEE Magn. Lett.* (2018) (to be published).
 - ⁴⁵ See Supplemental Material at [URL] for the simulation modeling details and more information regarding the current-driven motion and separation of monolayer skyrmions, and movies on current-induced skyrmion separation.
 - ⁴⁶ M. J. Donahue and D. G. Porter, Interagency Report NO. NISTIR 6376, National Institute of Standards and Technology, Gaithersburg, MD (1999) [<http://math.nist.gov/oommf/>].
 - ⁴⁷ W. Koshibae and N. Nagaosa, *Nat. Commun.* **7**, 10542 (2016).
 - ⁴⁸ X. Zhang, J. Xia, G. P. Zhao, X. Liu and Y. Zhou, *IEEE Tran. Magn.* **53**, 1 (2017).
 - ⁴⁹ L. Heyne, J. Rhensius, D. Ilgaz, A. Bisig, U. Rüdiger, M. Kläui, L. Joly, F. Nolting, L. J. Heyderman, J. U. Thiele and F. Kronast, *Phys. Rev. Lett.* **105**, 187203 (2010).
 - ⁵⁰ S. D. Pollard, L. Huang, K. S. Buchanan, D.A. Arena and Y. Zhu, *Nat. Commun.* **3**, 1028 (2012).